Ion transport characteristics in nanofiltration membranes: measurements and mechanisms

Noeon Park, Jaeweon Cho, Seungkwan Hong and Sangyoup Lee

ABSTRACT

Ion transport characteristics during nanofiltration (NF) were investigated by measuring effective osmotic pressure and diffusivity experimentally. Effective osmotic pressure and diffusivity were measured through lab-scale transport and diffusion tests. First, it was shown that the water flux across NF membranes decreased dramatically with increasing ionic strength because of the noticeable increase in effective osmotic pressure. Second, the results from transport experiments showed that the ion selectivity values, which were derived from the thermodynamic model, decreased with increasing ionic strength. Third, by analysing the data of measured osmotic pressure and diffusivity, it was demonstrated that the former and the latter increased and decreased, respectively, as ionic strength increased. The experimentally determined osmotic pressure across NF membranes was much lower than that calculated theoretically. At best, around 5% or less of the theoretical osmotic pressure was obtained under the experimental conditions investigated. The effective osmotic pressure and ion rejection decreased in the presence of nano-colloids. The influence of nano-colloids on ionic transport was found to be dependent on the concentration and size of the nano-colloids. Therefore, ion transport characteristics across NF membranes can be determined practically by measuring effective osmotic pressure and diffusivity as these reflect both feed water and membrane properties.

Key words | effective diffusivity, effective osmotic pressure, ion transport characteristics, nano-colloids, nanofiltration

Noeon Park
R&D Budget Coordination Division,
Korea Institute of Science and Technology Evaluation and Planning (KISTEP),
11F Dongwon Industry Bldg, 275,
Yangjae-dong, Seocho-gu,
Seoul 137-130,
South Korea

Jaeweon Cho
Department of Environmental Science and Engineering,
Gwangju Institute of Science and Technology (GIST),
1 Oryong-dong, Buk-gu,
Gwangju 500-712,
South Korea

Seungkwan Hong
Sangyoup Lee (corresponding author)
Department of Civil, Environmental & Architectural Engineering,
Korea University,
1, 5-ka, Anam-dong, Sungbuk-gu,
Seoul 136-713,
South Korea,
Tel.: +82-2-3290-3731;
Fax: +82-2-928-7656
E-mail: *sangyoup_lee@korea.ac.kr*

INTRODUCTION

The use of nanofiltration (NF) membranes with a nominal molecular weight cut-off (MWCO) ranging from 100 to 1,000 Dalton (Da) has rapidly increased in the field of separation and purification as NF could replace both reverse osmosis (RO) and ultrafiltration (UF) in certain cases (Al-Sofi *et al.* 2000; Cho *et al.* 2000; Kimura *et al.* 2003; Nghiem *et al.* 2004). Nanofiltration, as an advanced drinking water treatment process, can be applied for the efficient removal of natural organic matter (NOM) and micro-pollutants (i.e. disinfection by-products (DBPs), endocrine disrupting compounds (EDCs), and pharmaceutically active compounds (PhACs)). The removal efficiency of these compounds by NF membranes depends on the water chemistries (i.e. pH and ionic strength), membrane properties (i.e. surface charge, pore size, hydrophobicity and roughness) and operating conditions (i.e. temperature, recovery and trans-membrane pressure) (Braghetta *et al.* 1997; Hong & Elimelech 1997). However, either reversible or irreversible membrane fouling occurs during filtration, which dramatically reduces the membrane performance (Cho *et al.* 1998). Membrane fouling often results in the deterioration of product water quantity. In addition, it influences the quality of product water as the accumulation of foulants on the membrane surface affects the solute transport behaviour across the membranes.

One of the key features of NF membranes is to separate ions from water. The desalination of seawater has been

doi: 10.2166/aqua.2010.034

mainly performed using a reverse osmosis membrane and electrodialysis (Narayanan *et al.* 1991; Wilf & Bartels 2005). Recently, a series of NF membranes were operated economically for seawater desalination (Peeters *et al.* 1998). NF membranes showed considerable rejection of multivalent ions, but there was only moderate rejection for monovalent ions. The ion rejections by different NF membranes, however, have shown a wide range of values, implying that their rejection efficiency depends on the membrane properties (i.e. pore size and surface charge) since osmotic pressure and concentration polarization during filtration differ with respect to the membrane properties. An important factor in nanofiltration for efficient desalination of seawater is the osmotic pressure due to concentration differences, which are related to both the permeate flux and removal efficiency. The osmotic pressure was found to increase with increasing ionic strength, which simultaneously influenced the ion diffusive transport across the NF membrane pores (refer to *effective diffusivity*).

When the solute is impermeable and the solvent permeable to a selective membrane, the osmotic pressure is commonly calculated by the van't Hoff equation. The osmotic pressure is proportional to the solute concentration, but inversely proportional to the molecular size of the solute. However, experimental data including the water flux and solute rejection often significantly deviate from those obtained theoretically owing to the occurrence of external and internal concentration polarization (Mulder 1996; Moon *et al.* 2000). The membrane orientation in forward osmosis (FO) operations has also been found to influence the water flux and ion rejection efficiency (Gary *et al.* 2006; McCutcheon *et al.* 2006). In these studies, both concentrative and dilutive internal concentration polarizations (CP) have been investigated where a noticeable difference between theoretically calculated and experimentally obtained osmotic pressures (refer to *effective osmotic pressure*) existed.

The bulk diffusion coefficient for solutes can be calculated based on the Stokes-Einstein equation, while the effective (i.e. hindered) diffusion coefficient can be determined experimentally (Einstein 1956; Park *et al.* 2004). The Stokes-Einstein equation is a thermodynamic model, which assumes the following: (1) the type of solute is spherical; (2) there is no solute–solute interaction under dilute conditions; and (3) there is no resistance to solute transport in the bulk solution. The effective diffusion coefficient is a practical parameter in understanding the solute transport through membrane pores, which can be determined experimentally through diffusion cell tests (Wang *et al.* 2001). The effective diffusion coefficient of charged macromolecules increases with either decreasing pH or increasing ionic strength due to the compaction of the solute as well as the decrease in electrostatic repulsion (Wang *et al.* 2001). In addition, the presence of various nano-colloids including colloidal NOM and inorganic colloids in the aquatic environment has been assumed to affect ionic transport characteristics during RO and NF applications (Cho *et al.* 2006; Kwon *et al.* 2006). However, to date, the effective osmotic pressure and diffusivity during nanofiltration in the presence of nano-colloids has not been investigated.

The main objectives of this study were to: (1) determine the effective osmotic pressure and diffusivity across NF membrane pores; (2) assess the influence of nano-colloids on the effective osmotic pressure and diffusivity; and (3) evaluate the ionic transport characteristics across NF membrane pores considering membrane properties. Based on these investigations, the precise measurement methods for ion transport characteristics in NF membranes as well as mechanisms and factors involved are discussed.

MATERIALS AND METHODS

Measurements of effective osmotic pressure and diffusivity

A schematic diagram of the osmometer system used for measuring effective osmotic pressure and diffusivity across NF membrane pores is shown in Figure 1. The system consisted of a pump, membrane cell, temperature controller, tubing and glass flask. A rectangular type membrane cell, with symmetric channels on both sides of the membrane and dimensions of 9.6 (length) × 6.0 (width) × 0.05 cm (thickness), was employed.

The feed solution containing NaCl was allowed to flow into the feed side of the membrane cell, while pure water

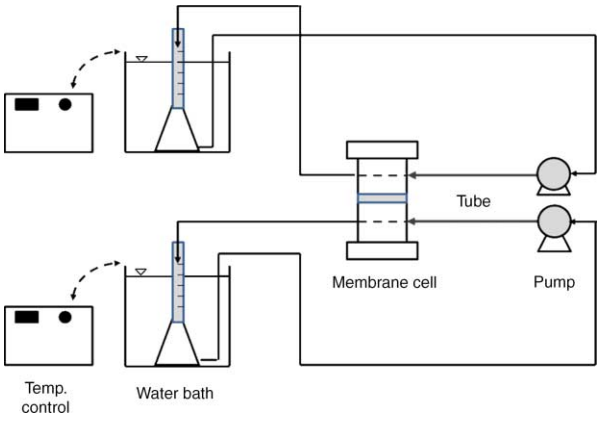

Figure 1 | Schematic diagram of the osmometer system designed in this study.

flowed into the permeate side of the cell. The circulation flow rate was 5 ml min^{-1} and the temperature was adjusted to be 25°C using a temperature controller. Prior to the experiments, the clean membrane was immersed in pure water and stored in a refrigerator (4°C) for 2 days, with the water replaced several times to remove the humectants. In addition, the influence of ionic concentration on the effective osmotic pressure and diffusivity was investigated in the presence of nano-colloids. The ionic concentrations on both sides of the chamber were measured using a conductivity meter (Cole Parmer, US). The volume of water moved from the permeate to the feed sides (i.e. dynamic osmotic volume) was monitored periodically by recording the height of water in the chambers. When there is no more change in the water height of the chambers, it can be assumed that the system has reached a dynamic (or semi-) equilibrium state, since there is still salt diffusive transport from the feed to the permeate. It should be noted that common NF membrane is not completely semi-permeable (i.e. water permeable/salt impermeable). Using the total changes in the height of the chambers at this state, the effective osmotic pressure was determined. The effective diffusivity across the NF membrane was calculated using Equation (1) based on Fick's first law (Tuwiner 1962; See & White 1999). The influence of nano-colloids with various sizes on the effective osmotic pressure and diffusivity was also investigated during nanofiltration.

$$\ln\frac{C_{P,t}-C_{F,t}}{C_{P,0}-C_{F,0}} = -\frac{AD_P}{l}\left[\frac{1}{V_F}+\frac{1}{V_P}\right]t \quad (1)$$

Here, C_F and C_P are the ionic concentrations in the feed and permeate chambers of the osmometer cell, respectively, A the membrane area, l the membrane thickness, V_F and V_P the volume of feed and permeate sides of the chamber, respectively, and t the diffusion test time.

Determination of ion transport across NF membranes

Ionic transport phenomena through NF membranes were investigated using an irreversible thermodynamic model. Kedem & Katchalsky (1958) developed a non-equilibrium model for both the solvent flux (J_v) and solute flux (J_s) based on irreversible thermodynamics. The solute flux was dominated by either diffusion or convection depending on operating conditions.

$$J_v = L_p(\Delta P - \sigma\Delta\pi) \quad (2)$$

$$J_s = \text{Diffusion} + \text{Convection} = \omega\Delta\pi + (1-\sigma)J_v C^* \quad (3)$$

Here, L_p, ΔP, and $\Delta\pi$ are the pure water permeability, trans-membrane pressure and osmotic pressure, respectively, and σ the reflection coefficient, having a value between 0 and 1. C^* ($C^* = (C_m - C_p)/\ln(C_m/C_p)$) is the mean logarithmic concentration between the membrane surface concentration (C_m) and the permeate concentration (C_p). ω is the solute permeability, which is driven by the concentration difference between C_m and C_p. The solute permeability (P_m) can also be obtained via:

$$\omega = \frac{P_m}{RT} = \frac{D_P}{lRT} \quad (4)$$

here, R, T and l are the gas constant, absolute temperature and total membrane thickness, respectively. The transport parameters, such as P_m and σ, were determined using a non-linear estimation method (Tandon *et al.* 1994) by the Statistica software by varying the trans-membrane pressure (Lee *et al.* 2004). The assumptions for developing the equation were, first, the membrane system was under steady-state conditions, second, there was no electrostatic interaction or pore wall effect and, third, the feed solution was under diluted conditions. More details on developing these transport models can be found in the previous studies (Tandon *et al.* 1994; Lee *et al.* 2004).

Salts, nano-colloids and NF membranes

Sodium chloride (Merck, Germany) solutions were prepared at concentrations of 5, 10, 20, 50, 100, 150 and 200 mM and used to determine the effective osmotic pressure and diffusivity across the NF membranes. Nano-scale polystyrene colloids, with sizes of 30, 60 and 90 nm, were obtained from Duke Scientific Corporation (US). The density of the polystyrene colloid was $1.05\,g\,cm^{-3}$. Various concentrations (i.e. 10, 16, 20, 30 and $50\,mg\,l^{-1}$) of the nano-colloids were employed.

Two different commercially available thin-film-composite (TFC) NF membranes, having similar pore size distributions, were used in this study (i.e. ESNA1-LF (Hydranautics, US) and HL (GE-Osmonics, US)). The molecular weight cut-off (MWCO) of the tested NF membranes, as determined by the fractional rejection method using non-charged polyethylene glycol (PEG) solutes (Lee *et al.* 2002), ranged from 300 to 600 Da. The manufacturer reported that meta-phenylene diamine (MPD) and piperazine, as water soluble monomers, have been used for the syntheses of the ESNA1-LF and HL membranes, respectively. The tested NF membranes showed hydrophilic properties based on contact angle measurements (Rame-Hart Inc., US). The ESNA1-LF membrane showed relatively lower pure water permeability compared with the HL membrane, implying the membrane resistance of the ESNA1-LF membrane was relatively greater than that of the HL membrane (see Table 1). A detailed description of membrane characterization methods can be found elsewhere (Brant & Childress 2002; Lee *et al.* 2002).

The zeta potentials of the tested NF membranes were determined by the electrophoretic method (Shim *et al.* 2002). The electro-mobility of coated latex particles, with a diameter of 520 nm, was measured using a light scattering method, and the zeta potentials of the tested membranes were simultaneously calculated based on the Smoluchowski equation. Prior to zeta potential measurements, NF membranes were soaked in salt solution for adsorption equilibrium. The zeta potentials of nano-colloids were measured in a similar way. The highly concentrated nano-colloids solution was replaced with coated latex particles for measuring the zeta potential of the nano-colloids. The zeta potential was determined by varying the ionic strength at a constant pH of 6.0. As shown in Figure 2, negative and neutral surface charges were obtained for the ESNA1-LF and HL membranes, respectively. As the ionic strength of the solution increased, the zeta potential of the tested NF membranes decreased toward neutral charges, as a result of double layer compaction. A 30 nm nano-colloid showed a relatively higher negative surface charge compared with the tested NF membranes. The zeta potential measurements were conducted in triplicate, with the average values used in this study.

Lab-scale filtration tests

A pressure-driven crossflow filtration test unit was used, containing a rectangular type cell, with a length and width of 9.6 and 6.0 cm, respectively, and feed spacer thickness of 0.05 cm. The filtration test unit was composed of a membrane cell, feed reservoir, pump and temperature controller. The temperature was maintained at 25°C using the temperature controller with stainless coil immersed in the feed water (Polyscience, US). The feed flow rate was $500\,ml\,min^{-1}$, with the permeate flow rate maintained at $4.5\,ml\,min^{-1}$ by adjusting the pump speed and retentate valve. This was required because the pure water permeability of each membrane was different. Both the permeate flux and trans-membrane pressure were monitored using a digital flow meter (Optiflow-1000, Agilent, US) and digital pressure meter (Konics Co., Korea), respectively, interfaced to a computer. The concentrations of NaCl solution for the filtration experiments were 10, 20,

Table 1 | Membrane properties

Code	Manufacturer	Material	MWCO	Contact angle (°)	Pure water permeability (l/day-kPa-m^2)
ESNA1-LF	Hydranautics, USA	Polyamide TFC (MPD)	300–600	50 ± 1.5	1.8
HL	GE-Osmonics, USA	Polyamide TFC (Piperazine)	300–600	15 ± 2.0	3.9

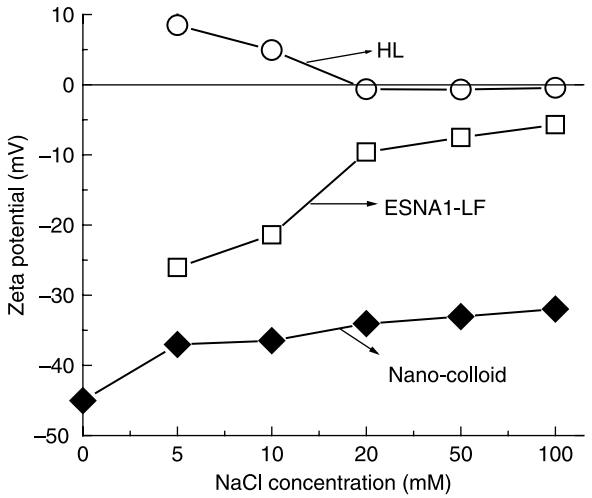

Figure 2 | Zeta potentials of the NF membranes and nano-colloids as a function of NaCl concentration (pH 6.0).

50 and 100 mM. The ionic concentrations on the feed and permeate sides were measured using a conductivity meter. The membrane performance, including water flux and ion rejection efficiency was also investigated either in the absence or in the presence of 10 mg l^{-1} nano-colloids.

Lab-scale ion transport tests

The crossflow filtration test unit was used for ion transport experiments. The operating conditions (i.e. temperature, feed flow rate and dimensions of membrane cell) for the transport experiments were similar to those for the filtration experiments described in the previous section. The trans-membrane pressures were varied from 30 to 110 psi by adjusting the pump speed and retentate valve. The permeate flux and ion rejection were monitored at various trans-membrane pressures. Transport parameters, such as P_m and σ, were calculated by plotting the observed rejection (R_{obs}) against the permeate flux (J_v) obtained from the transport experiments through a linear regression method (Lee *et al.* 2004).

RESULTS AND DISCUSSION

Influence of ionic strength on permeability and rejection

The influence of feed solution ionic strength on water permeability was investigated with two NF membranes and the results are shown in Figure 3. As shown in Figure 3, the water flux decreased dramatically with increasing ionic strength owing to the increase in osmotic pressure. The permeability reduction of the ESNA1-LF membrane with respect to ionic strength was much greater than that of the HL membrane. For the ESNA1-LF membrane, the water permeability obtained at the ionic strength of 100 mM decreased by up to 60% (see open symbols in Figure 3(a)) compared with the flux obtained at 10 mM ionic strength, while the HL membrane exhibited a 30% or less flux reduction (see open symbols in Figure 3(b)) at the same condition. This was due to the fact that the osmotic pressure difference across the ESNA1-LF membrane was much higher than that of the HL membrane as the physicochemical properties of two membranes are different (note that other experimental conditions are identical except the membranes employed). The ion rejection by the ESNA1-LF membrane was nearly 70% at 100 mM (see closed symbols in Figure 3(b)), while that by the HL membrane

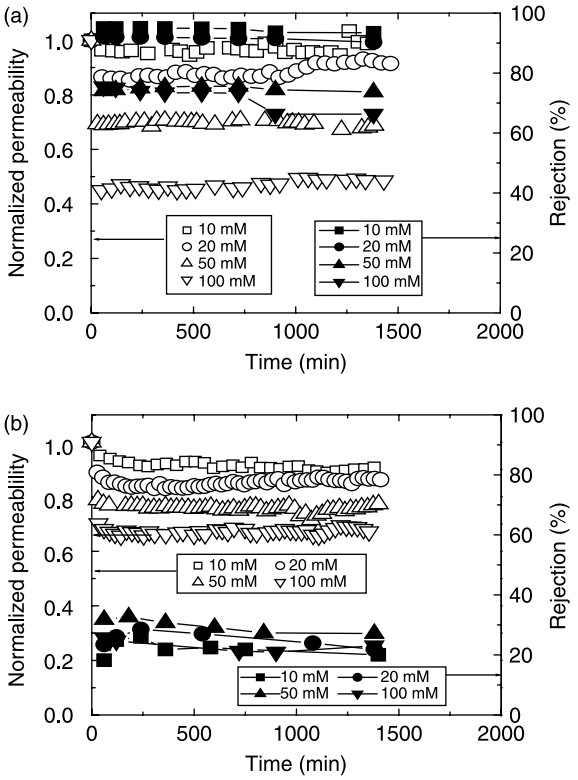

Figure 3 | Normalized water permeability (open symbols) and ion rejection (closed symbols) at different feed water NaCl concentrations: (a) ESNA1-LF and (b) HL. Normalization was carried out based on pure water permeability.

was about 20% (see closed symbols in Figure 3(b)). Since the MWCO of both membranes are almost identical, these differences (i.e. water permeability as well as ion rejection upon ionic strength variation) are mainly attributed to the lower negative surface charge, hydrophobicity and hydraulic resistance of the HL membrane (see Table 1 and Figure 2).

The membrane performance in terms of ion rejection in the presence of 30 nm nano-colloids was investigated and the results are shown in Figure 4. The concentration of nano-colloids in feed solution was 10 mg l^{-1}. The influence of nano-colloids on ion rejection by the ESNA1-LF membrane was almost negligible (see Figures 3(a) and 4(a)), while that by the HL membrane noticeably decreased

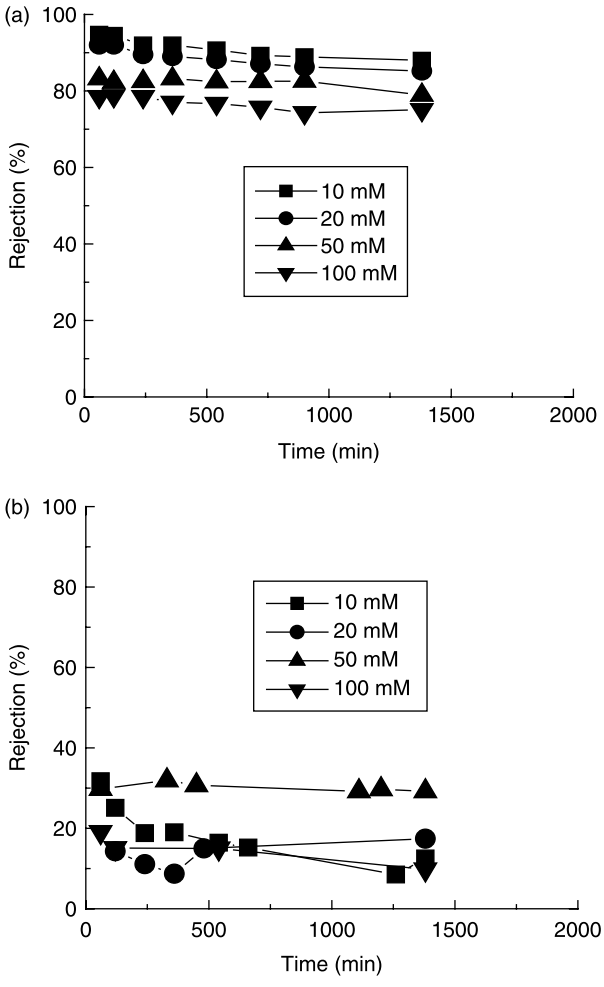

Figure 4 | Influence of nano-colloids (30 nm, 10 mg l^{-1}) on ion rejection at different feed water NaCl concentrations: (a) ESNA1-LF and (b) HL.

in the presence of nano-colloids exhibiting ion rejection of less than 20% at the higher ionic strengths (see Figures 3(b) and 4(b)). This can be attributed to the accelerated diffusive transport of ions across the membranes. Thick and dense colloidal cake layer formed by the favourable accumulation of nano-colloids on the neutrally charged HL membrane surface hindered the back diffusive transport of ions away from the membrane surface and, thus, the increase in ion concentration on the membrane surface. This mechanism is often called 'cake-enhanced osmotic pressure' and similar trends of accelerated transmission of ions across the membrane in the presence of colloidal particles have been reported previously (Kuberkar & Davis 2000; Vrijenhoek *et al.* 2001; Lee *et al.* 2005). Negatively charged nano-colloids with a relatively low concentration (i.e. 10 mg l^{-1}) are unfavourable for the formation of a thick and dense cake layer as the ESNA1-LF membrane with strong negative surface charge prevents nano-colloid deposition on the membrane surface. This implies that the presence of nano-colloids during water treatment by NF membranes could affect the membrane performance (i.e. ion rejection as well as flux decline), especially when the membranes employed are favourable to colloidal deposition.

Determination of transport parameters (P_m, σ and D_p)

Ion transport experiments using the NF membranes were performed by varying the trans-membrane pressure. The crossflow velocity was controlled to be the same value (i.e. 8.5 cm s^{-1}) at each trans-membrane pressure. Based on the experimental results, the related intrinsic membrane transport parameters (P_m and σ) were calculated using Equation (3). The values are listed in Table 2. Figure 5 shows the variation of observed rejection (R_{obs}) by the NF membranes with respect to the trans-membrane pressure at various ionic strengths. The ion transmission through the HL membrane (see Figure 5(b)) was much higher compared with the ESNA1-LF membrane. The ion rejection by the ESNA1-LF membrane was not significantly affected by the trans-membrane pressure, while the HL membrane showed a noticeable increase in the ion rejection with increasing trans-membrane pressure. This shows that the acceleration of convective water flux caused by the increase in trans-membrane pressure is more favourable in the HL

Table 2 | Ionic transport parameters and effective diffusivity determined based on the thermodynamic model

	ESNA1-LF			HL		
	P_m ($\times 10^{-6}$, cm s^{-1})	D_p ($\times 10^{-7}$, cm^2 s^{-1})	σ	P_m ($\times 10^{-6}$, cm s^{-1})	D_p ($\times 10^{-7}$, cm^2 s^{-1})	σ
10 mM	1.3	0.3	0.8	70.0	16.1	0.3
20 mM	10.8	2.1	0.8	78.2	18.0	0.1
50 mM	7.8	1.5	0.7	86.7	19.9	0.1
100 mM	8.9	1.7	0.6	59.5	13.7	0.1

membrane compared with the ESNA1-LF membrane and, thus, the apparent increase in ion rejection due to the dilution effect (Lee *et al.* 2004). In both cases, however, the ion rejection by the NF membranes decreased with increasing ionic strength.

From a practical point of view, the NF membrane performance in terms of salt rejection could vary depending on feed water sources (i.e. seawater, brackish water, surface water and wastewater) which have quite different salt contents. By applying the experimental data shown in Figure 5 to Equation (3), it was found that the P_m (i.e. solute permeability) for the ESNA1-LF membrane was much smaller than that for the HL membrane (see Table 2). This is well in accordance with the rejection data shown in Figure 3 (i.e. in the absence of nano-colloids). The effective ionic diffusivity (D_p) across the membrane pores was calculated by substituting the solute permeability (P_m) into Equation (4) (see Table 2). Note that the total thicknesses (l) of the ESNA1-LF and HL membranes were 0.019 and 0.023 cm, respectively. The D_p for the ESNA1-LF membrane was also much smaller than that for the HL membrane. This indicates that both the ion rejection efficiency and selectivity (σ) for the ESNA1-LF membrane are much higher than those for the HL membrane. As listed in Table 2, the selectivity (σ) decreased with increasing ionic strength, while the effective diffusivity (D_p) showed no distinct relation to the ionic strength.

The effect of nano-colloids on the ionic transport characteristics of the NF membranes is depicted in Figure 6. As shown in Figure 6, the ion rejection by the HL membrane decreased by approximately 30% at 100 psi in the presence of nano-colloids, while the influence of nano-colloids on ion rejection by the ESNA1-LF membrane was almost negligible. This was also in good agreement with the previous results obtained from the filtration experiments (see Figures 3 and 4) showing the accelerated transmission of ions due to the increase in ion concentration at the membrane surface in the presence of nano-colloids.

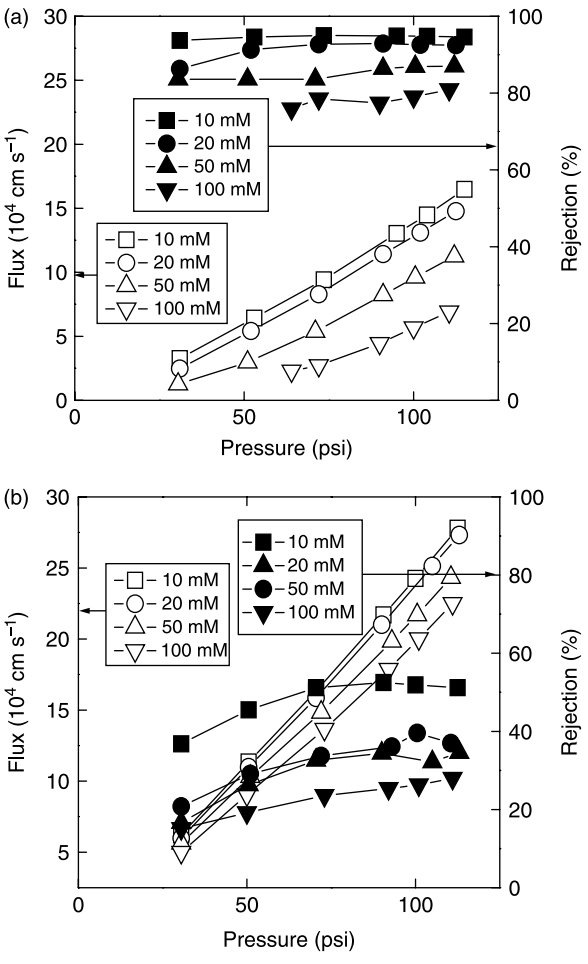

Figure 5 | Ion rejection with respect to trans-membrane pressures at different feed water NaCl concentrations: (a) ESNA1-LF and (b) HL.

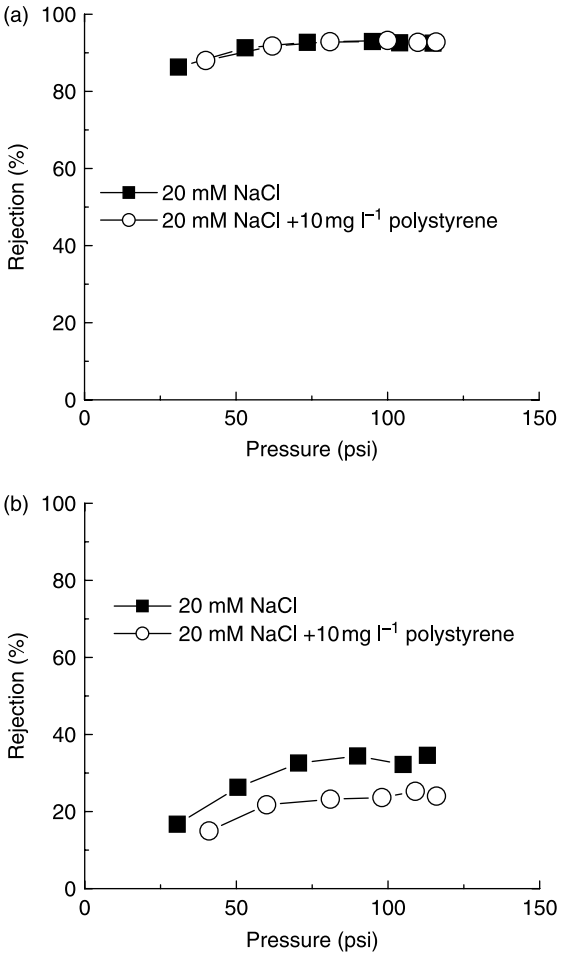

Figure 6 | Ion rejection with respect to trans-membrane pressure in the presence of nano-colloids (30 nm, 10 mg l^{-1}): (a) ESNA1-LF and (b) HL.

Effective osmotic pressure and diffusivity

The ionic transport characteristics across NF membrane pores were experimentally investigated by measuring the effective osmotic pressure and diffusivity using the osmometer system. Theoretically (i.e. van't Hoff equation) and experimentally (i.e. transport and diffusion tests) derived osmotic pressures were compared with respect to ionic strength. The results are listed in Table 3. The ESNA1-LF membrane exhibited a much higher effective ionic osmotic pressure (i.e. order of magnitude) than the HL membrane, while the theoretical values are similar for both membranes. This provides a good explanation of the previous experimental data of visible differences in water permeability and ion rejection of the two membranes. The theoretical to experimental osmotic pressure ratio deviated significantly from the value of 1.0, as ions could be transmitted through the membrane pores and, thus, both external and internal concentration polarization occurred.

More obvious deviation (i.e. $\Delta\pi_{theo}$ and $\Delta\pi_{exp}$) for HL membranes can be explained by the solute permeability data listed in Table 2 where the P_m values for the HL membranes are nearly 10 times higher than those for the ESNA1-LF membranes. In addition, as the ionic concentration increased, this ratio gradually decreased because of the increasingly severe internal and external concentration polarizations. Furthermore, the effective osmotic pressure is governed by the internal concentration polarization (ICP) rather than the external concentration polarization (ECP) owing to the thicker porous support layer of common thin-film-composite membranes. Thus, the mass transfer coefficient for the ECP is not enough to explain this difference. At best, around 5% or less of the theoretical osmotic pressure was obtained under the experimental conditions investigated. It may be noted that the difference between $\Delta\pi_{theo}$ and $\Delta\pi_{exp}$ could be much smaller for the membranes with more than 99% salt rejection such as RO membranes (i.e. the selectivity (σ) of RO membranes is commonly assumed to be 1.0).

Similar data to those shown in Table 3 were determined by the transport and diffusion experiments in the presence of nano-colloids. The results are listed in Table 4. The results showed that the effective osmotic pressure in the presence of nano-colloids decreased slightly for both membranes compared with the experimental data shown in Table 3 (i.e. in the absence of nano-colloids), except for the salt concentration of 150 mM. In addition, the theoretical to experimental osmotic pressure ratios were substantially decreased for both membranes. This can be explained by the supposition that the net osmotic pressure across the NF membrane decreased in the presence of nano-colloids as a result of either ionic adsorption on colloid surface or ionic restriction by colloidal clusters at high ionic strengths. In both cases, the net amount of ions available to produce osmotic pressure tends to decrease.

Effective diffusivity across the membrane pores determined under different conditions is listed in Table 5. The effective diffusivity slightly decreased with increasing ionic strength, possibly because of the reduction in the

Table 3 | Comparison between the osmotic pressures calculated by the van't Hoff Equation ($\Delta\pi_{theo}$) and that determined experimentally using the osmometer system ($\Delta\pi_{exp}$) in the absence of nano-colloids (30 nm, 10 mg l^{-1})

	ESNA1-LF				HL			
Feed conc. (mM)	ΔC (mM)	$\Delta\pi_{theo}$ (atm)	$\Delta\pi_{exp}$ (atm)	$\Delta\pi_{exp}/\Delta\pi_{theo(\%)}$	ΔC (mM)	$\Delta\pi_{theo}$ (atm)	$\Delta\pi_{exp}$ (atm)	$\Delta\pi_{exp}/\Delta\pi_{theo}$ (%)
5	4.4	0.2	0.010	4.9	–	–	–	–
10	8.6	0.4	0.014	3.3	9.4	0.4	0.002	0.6
20	12.8	0.6	0.026	4.1	10.4	0.5	0.002	0.5
50	33.9	1.7	0.037	2.2	22.5	1.1	0.006	0.6
100	84.7	4.1	0.051	1.2	65.4	3.2	0.008	0.3
150	127.4	6.2	0.063	1.0	85.4	4.2	0.007	0.2

–, no data available.

membrane pore size as a result of polymer matrix compaction at high ionic strengths. The ion-binding interaction at high ionic concentrations was also affected, implying a reduction in ion activity. Furthermore, the ion movements across the pores could be influenced by the osmotic pressure. The effective diffusivities for the ESNA1-LF membrane were almost similar regardless of nano-colloids. However, the ionic diffusivity for the HL membrane increased the most. These observations are well in accordance with previous results showing less ion rejection with the addition of nano-colloids for the HL membranes (see Figures 3(b) and 4(b)). This could explain the much higher ion rejection by the ESNA1-LF membranes compared with the HL membranes even though these membranes exhibited similar MWCO values. It was quite noticeable that the ionic diffusivities (D_p) obtained from the transport experiments (i.e. Table 2) were quite similar to those determined by the diffusion test using the osmometer system (i.e. Table 5) at each corresponding ionic strength.

Influence of concentration and size of nano-colloids on ion transport characteristics

It has been shown that the presence of nano-colloids during NF of ionic solution could affect the ion transport characteristics and, hence, the alteration of membrane performance (i.e. water permeability and ion rejection). In this section, various nano-colloids with different sizes and concentrations were used to investigate how colloidal size and concentration affect the ion transport characteristics (i.e. effective osmotic pressure). The results are shown in Figure 7 where the dynamic osmotic volume (i.e. Y-axis) is directly proportional to the effective osmotic pressure; the driving force for volume changes in the osmometer system is the effective osmotic pressure. In Figure 7(a), the influence of the nano-colloid concentration on the effective osmotic pressure for ESNA1-LF membrane is depicted. The effective osmotic pressure for the ESNA1-LF membrane decreased with increasing nano-colloid concentration at an ionic strength of 20 mM. This supports the previous

Table 4 | Comparison between the osmotic pressures calculated by the van't Hoff Equation ($\Delta\pi_{theo}$) and that determined experimentally using the osmometer system ($\Delta\pi_{exp}$) in the presence of nano-colloids (30 nm, 10 mg l^{-1})

ESNA1-LF					HL			
Feed conc. (mM)	ΔC (mM)	$\Delta\pi_{theo}$ (atm)	$\Delta\pi_{exp}$ (atm)	$\Delta\pi_{exp}/\Delta\pi_{theo(\%)}$	ΔC (mM)	$\Delta\pi_{theo}$ (atm)	$\Delta\pi_{exp}$ (atm)	$\Delta\pi_{exp}/\Delta\pi_{theo}$ (%)
10	7.9	0.4	0.010	2.5	5.11	0.2	0.001	0.3
20	10.5	0.5	0.017	3.3	18.2	0.9	0.001	0.1
50	15.1	0.7	0.022	3.0	46.7	2.3	0.001	0.1
100	48.6	2.4	0.028	1.2	78.0	3.8	0.001	0.1
150	57.2	2.8	0.082	2.9	128.1	6.3	0.003	0.1
200	–	–	–		153.9	7.5	0.008	0.1

Table 5 | Effective ionic diffusivity determined experimentally

D_p ($\times 10^{-7}$, $cm^2 s^{-1}$)		20 mM	50 mM	100 mM	150 mM
ESNA1-LF	NaCl	3.0	3.0	3.0	1.9
	NaCl + nano-colloids	3.9	4.3	2.1	1.1
HL	NaCl	16.5	16.5	12.7	12.0
	NaCl + nano-colloids	16.4	17.4	15.7	10.2

supposition that ion adsorption or restriction could affect the effective osmotic pressure as these ion–colloid interactions are more favourable at the higher colloid concentrations. However, the effect of nano-colloid concentrations higher than $16\,mg\,l^{-1}$ was similar. This is because the electrostatic interactions (i.e. ion adsorption or restriction) between the ions and nano-colloids had already been saturated. The effect of nano-colloid size on the effective osmotic pressure is shown in Figure 7(b). All experiments were conducted with a nano-colloid concentration of $10\,mg\,l^{-1}$. It was shown that the dynamic osmotic volume (i.e. proportional to the effective osmotic pressure) was much higher for the greater size of nano-colloids. The reason for this observation is the greater specific surface area of the smaller colloids compared with the larger colloids. Colloidal adsorption as well as restriction increases as the specific surface area of nano-colloids increases.

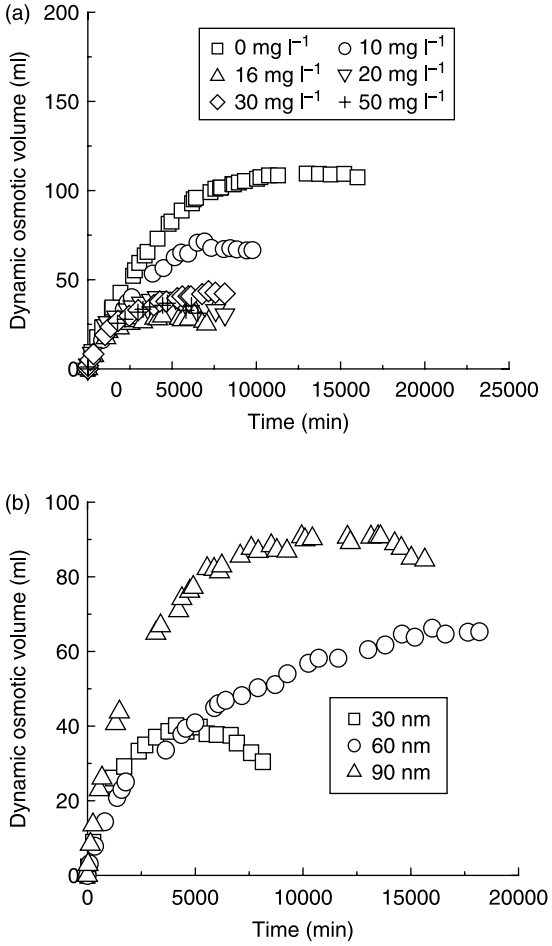

Figure 7 | Influence of (a) concentration and (b) size of nano-colloids on dynamic osmotic volume (i.e. experimentally determined water volume flowing from permeate to feed sides) for ESNA1-LF membrane.

CONCLUSIONS

In this study, the ionic transport characteristics in NF membranes were systematically investigated by analysing individually obtained experimental data from the filtration, transport and diffusion tests. Membrane filtration tests were performed by varying the ionic strength of the feed water. The permeability and ion rejection were significantly reduced with increasing ionic strength, which was related to the changes in the membrane pore size, ion binding interactions and the electro-osmotic effect. The ion rejection by the ESNA1-LF membrane was not significantly affected by the presence of nano-colloids, while that by the HL membrane decreased noticeably. This was attributed to hindrance of the ionic diffusivity. The overall ion rejection efficiency by the ESNA1-LF membrane was higher than that of the HL membrane with a similar MWCO, as a result of the smaller ionic diffusivity and negative surface charge of the ESNA1-LF membrane, implying that both feed water and membrane properties affect the membrane performance in terms of water permeability and ion rejection. Transport experiments were performed to investigate the ionic transport characteristics. The R_{obs} of the NF membranes decreased with increasing ionic strength. The selectivity of ions (i.e. calculated based on the thermodynamic model) also decreased with increasing ionic strength.

It was demonstrated that the measurement of effective osmotic pressure and diffusivity allows precise understanding of ion transport characteristics along with the mechanisms involved. The effective osmotic pressure across

the NF membrane pores decreased with either a lower ionic strength or the presence of nano-colloids. The theoretical osmotic pressure calculated from the van't Hoff equation was overestimated since the pore sizes of the tested NF membranes were much larger than those of the ions; also, both external and internal concentration polarization occurred. The lower ion rejection by the HL membrane resulted from its higher effective diffusivity. The effective osmotic pressure was observed to be dependent on the concentration and size of the nano-colloids. Overall, it can be concluded that ion transport across a salt-rejecting membrane is mainly governed by the effective osmotic pressure and diffusivity rather than theoretical values especially for NF membranes compared with RO membranes. In addition, both feed water quality (i.e. presence of nano-colloids) and membrane properties (i.e. surface charge and hydraulic resistance) are key factors affecting the ion transport characteristics.

ACKNOWLEDGEMENTS

This research was supported by a grant from the National Research Laboratory Program (NRL) of the Korea Science and Engineering Foundation (NOM ecology Lab: R0A-2007-000-20055-0) and Korea University grant.

REFERENCES

Al-Sofi, M. A. K., Hassan, A. H., Hamed, O. A., Dalvi, A. G. I., Kither, M. N. M., Mustafa, G. M. & Bamardouf, K. 2000 Optimization of hybridized seawater desalination process. *Desalination* **20**, 147–156.

Braghetta, A., DiGiano, F. A. & Ball, W. P. 1997 Nanofiltration of natural organic matter: pH and ionic strength effects. *J. Environ. Eng.* **123**(7), 628–640.

Brant, J. A. & Childress, A. E. 2002 Assessing short-range membrane-colloid interactions using surface energetics. *J. Memb. Sci.* **203**, 257–273.

Cho, J., Amy, G., Pellegrino, J. & Yoon, Y. 1998 Characterization of clean and natural organic matter fouled NF and UF membranes, and foulants characterizations. *Desalination* **118**, 101–108.

Cho, J., Amy, G. & Pellegrino, J. 2000 Membrane filtration of natural organic matter: factors and mechanisms affecting rejection and flux decline with charged ultrafiltration (UF) membrane. *J. Memb. Sci.* **164**, 89–110.

Cho, J., Park, Y., Sun, H., Kim, S. & Yoon, Y. 2006 Measurements of effective sizes and diffusivities of nano-colloids and micro-particles. *Colloids Surf. A* **274**(1–3), 43–47.

Einstein, A. 1956 *Investigations of the Theory of the Brownian Movement*. Dover Publication Inc, New York.

Gary, G., McCutcheon, J. R. & Elimelech, M. 2006 Internal concentration polarization in forward osmosis: role of membrane orientation. *Desalination* **197**, 1–8.

Hong, S. K. & Elimelech, M. 1997 Chemical and physical aspects of natural organic matter (NOM) fouling of nanofiltration membranes. *J. Memb. Sci.* **132**, 159–181.

Kedem, O. & Katchalsky, A. 1958 Thermodynamic analysis of the permeability of biological membranes to non-electrolytes. *J. Biochem. Biophys. Acta* **27**, 229–246.

Kimura, K., Amy, G., Drewes, J. E., Heberer, T., Kim, T. & Watanabe, Y. 2003 Rejection of organic micropollutants (disinfection by-products, endocrine disrupting compounds, and pharmaceutically active compounds) by NF/RO membranes. *J. Memb. Sci.* **227**, 113–121.

Kuberkar, V. T. & Davis, R. H. 2000 Modeling of fouling reduction by secondary membranes. *J. Memb. Sci.* **168**, 243–258.

Kwon, B., Cho, J., Park, N. & Pellegrino, J. 2006 Organic nanocolloid fouling in UF membranes. *J. Memb. Sci.* **279**(1–2), 209–219.

Lee, S., Park, G., Amy, G., Hong, S. K., Moon, S. H., Lee, D. & Cho, J. 2002 Determination of membrane pore size distribution using the fractional rejection of nonionic and charged macromolecules. *J. Memb. Sci.* **201**, 191–201.

Lee, S., Amy, G. & Cho, J. 2004 Applicability of Sherwood correlations for natural organic matter (NOM) transport in nanofiltration (NF) membranes. *J. Memb. Sci.* **240**(1–2), 49–65.

Lee, S., Elimelech, M. & Cho, J. 2005 Combined influence of natural organic matter (NOM) and colloidal particles on nanofiltration membrane fouling. *J. Memb. Sci.* **262**(1–2), 27–41.

McCutcheon, J. R., McGinnis, R. L. & Elimelech, M. 2006 Desalination by ammonia-carbon dioxide forward osmosis: influence of draw and feed solution concentrations on process performance. *J. Memb. Sci.* **278**, 114–123.

Moon, Y. U., Anderson, C. O., Blanch, H. W. & Prausnitz, J. M. 2000 Osmotic pressures and second virial coefficients for aqueous saline solutions of lysozyme. *Fluid Phase Equilib.* **168**, 229–239.

Mulder, M. 1996 *Basic Principles of Membrane Technology*. Kluwer Academic Publishers, New York.

Narayanan, P. K., Thampy, S. K., Dave, N. J., Chauhan, D. K., Makwana, B. S., Adhikary, S. K. & Indusekhar, V. K. 1991 Performance of the first sea water electrodialysis desalination plant in India. *Desalination* **84**(1–3), 201–211.

Nghiem, L. D., Schaefer, A. I. & Elimelech, M. 2004 Removal of natural hormones by nanofiltration membranes: measurement, modeling, and mechanisms. *Environ. Sci. Technol.* **38**, 1888–1896.

Park, N., Yoon, Y., Moon, S. H. & Cho, J. 2004 Evaluation of the performance of tight-UF membranes with respect to NOM removal using effective MWCO, molecular weight, and apparent diffusivity of NOM. *Desalination* **164**, 53–62.

Peeters, J. M. M., Boom, J. P., Mulder, M. H. V. & Strathman, H. 1998 Retention measurement of nanofiltration membranes with electrolytes solutions. *J. Memb. Sci.* **145**, 199–209.

See, D. M. & White, R. E. 1999 A simple method for determining differential diffusion coefficients from aqueous diaphragm cell data at temperatures below 0°C. *J. Electrochem. Soc.* **146**(2), 677–679.

Shim, Y., Lee, H. J., Lee, S., Moon, S. H. & Cho, J. 2002 Effects of natural organic matter and ionic species on membrane surface charge. *Environ. Sci. Technol.* **36**, 3864–3871.

Tandon, A., Gupta, S. K. & Agarwal, G. P. 1994 Modelling of protein transmission through ultrafiltration membranes. *J. Memb. Sci.* **97**, 83–90.

Tuwiner, S. B. 1962 *Diffusion and Membrane Technology*. Reinhold Publishing Corporation, New York.

Vrijenhoek, E., Hong, S. & Elimelech, M. 2001 Influence of membrane surface properties on initial rate of colloidal fouling of reverse osmosis and nanofiltration membranes. *J. Memb. Sci.* **188**, 115–128.

Wang, Y., Combe, C. & Clark, M. M. 2001 The effects of pH and calcium on the diffusion coefficient of humic acid. *J. Memb. Sci.* **183**, 49–60.

Wilf, M. & Bartels, C. 2005 Optimization of seawater RO systems design. *Desalination* **173**(1), 1–12.

First received 30 April 2009; accepted in revised form 13 November 2009